Egypt. J. Chem. **Vol. 65**, No. 9 pp. 389 - 404 (2022)

Egyptian Journal of Chemistry

http://ejchem.journals.ekb.eg/

Copper and Lead Ions Removal from Aqueous Solutions Case Study: Fly Ash Carbon as Low-Cost Effective Sorbent

E.M.Abdel Rahman[1], G.M.El-Subruiti[2], A.H.Kamel[3], H.M.Diab[1], S.S.M.Hassan,[3]
[1]*Central Laboratory for Environmental Radioactivity Measurements Inter-Comparison and Training (CLERMIT), Nuclear and Radiological Regulatory Authority, Cairo, Egypt*
[2]*Chemistry Department, Faculty of Science, Alexandria University, Alexandria, Egypt*
[3]*Chemistry Department, Faculty of Science, Ain Shams University, Cairo, Egypt*

Abstract

In this study, the use of fly ash for removal of copper (II) and lead (II) ions from aqueous solutions has been studied. The removal was conducted in batch system under various conditions of pH, contact time, initial concentration of metal ions, adsorbent dose and temperatures. Isotherms from Langmuir, Freundlich, and Dubinin-Radushkevich at different temperatures (303-333 ^oK) were evaluated and the results were compared. Both pseudo-first and pseudo-second-order adsorption kinetics were also tested. Thermodynamic parameters; $\Delta H°$, $\Delta G°$, and $\Delta S°$ are calculated. SEM is used to assess morphological changed in the fly ash surfaces following adsorption of copper lead ions. The obtained results showed an equilibrium within 20 min and maximum adsorption and removal of 95 -100% of the metal ions at pH 6-7. The pseudo-second order adsorption model was found to be more suitable for describing the adsorption kinetics. Langmuir adsorption model displayed the best R_L values for copper ions adsorption ranged from 2.5 to 10.1 and lead ions adsorption ranged from 0.23 to 1.06. The Freundlich value of $1/n$ was less than 1, indicating favorable adsorption process and confirming adsorbent's heterogeneity. The thermodynamic parameters (ΔG, ΔH, ΔS) were found to be in the range of -502 to -1424 kJ/mol, -4.5 kJ/mol and 16.6 kJ/mol, respectively for copper and from -1525 to -3236 kJ/mol, -1.052 kJ/mol and 3.675 kJ/mol for lead ions. The mean free energy for copper was 0.002 kJ/mol, and for lead 0.0007 kJ/mol, confirming a physical adsorption mechanism.

Keywords: Fly ash, kinetic and thermodynamic adsorption, removal of copper and lead from aqueous solutions, scanning electron microscopy.

---

1. Introduction

Water contamination with heavy metals from wastewater discharges is one of the most critical problems associated with health hazard, as these pollutants are not-biodegradable, toxic and tend to be accumulated in living organisms [1]. Heavy metal ions removal from wastewater is an important step for improving water quality and to provide healthy water supply [2]. Therefore, before discharging into the environment, it is important to extract and remove these metal ions [3]. Copper and lead are considered the most toxic metals that affect the environment according to the World Health Organization report [4]. Several studies have been carried out to identify a suitable and cheap sorbent for heavy metal ions removal e.g., natural inorganic materials, peat, peat In the present work, fly ash is used as an efficient adsorbent for removing some toxic metal ions. Experimental conditions are optimized for maximum removal of lead and copper ions from aqueous solutions, and to convert fly ash from a useless hazardous substance to a useful substance for suitable removing of hazardous metal ions for wastewater.

2. Experimental

2.1. Chemicals

Analar grade copper(II) sulfate penta hydrate, and lead (II) acetate, (Adwic Chemicals, Egypt) and bi-distilled water were used for the preparation of copper and lead metal ion test solutions. Atomic absorption spectrometer (Perkin-Elmer 2380) was used for metal assessment. Fly ash was collected from a local power stations at (El-Zawia).

---

*Corresponding author e-mail: ehabmosa2020@gmail.com

Received date 09 October 2021; revised date 13 January 2022; accepted date 25 January 2022
DOI: 10.21608/EJCHEM.2022.100256.4657

Hydrochloric acid and sodium hydroxide were used for adjusting the pH of the test solutions.

2.2. Measurement of copper and lead

Dragon digital (hotplate) with a magnetic stirrer MS-H-Pro and temperature sensor PT 1000; IKA®KS4000i control was used. Copper and lead solutions (250-ml) were withdrawn and placed in a storage tank. The solutions were injected into a Perkin-Elmer 2380 atomic absorption spectrometer adjusted at ƛ = 324.8 nm for measuring copper ions and at ƛ = 232.0 nm for measuring lead ions. HI2211 pH/ORP meter HANNA instruments was used for pH adjustment of the test solutions.

2.3. Procedure

Adsorption experiments were carried out with copper and lead solutions adjusted to pH values ranging from 2 to 8 using hydrochloric acid and/or sodium hydroxide. The solutions were tested at different contact times (3, 5, 10, 15, 20 and 30 min), initial copper and lead ions concentrations (50, 100, 150,200 and 300 mg/l), fly ash carbon dosages (0.5, 1.0, 1.5, 2.0 and 2.5 g/l) and temperatures (303, 313,323 and 333^{o}K). The test solutions were taken at regular time intervals, filtered to separate the fly ash particulates and measuring the concentration of the metal ions using atomic absorption spectrometry. The data were used to calculate the equilibrium adsorption capacity q_e (mg/g) which is the difference between the initial and equilibrium metal concentrations, and q_t (mg/g) which is the difference between the initial and time changes (t) of metal concentrations:

$$\boldsymbol{q_e} = \frac{(Co-Ce)V}{\mathbf{m}} \qquad (1)$$

$$\boldsymbol{q_t} = \frac{(Co-Ct)V}{m} \qquad (2)$$

Metal removal (%), was determined from the equation:

$$\%\ \mathbf{Removal} = \frac{Co-Ct}{Co}\ \mathbf{x\ 100} \qquad (3)$$

Where C_o (mg/l) is the initial metal ions concentration in the test solution, C_e (mg/l) is the equilibrium concentration of the metal ions in the solution. C_t (mg/l) is the metal concentration in the solution after time (t), m is the used mass of fly ash used (g) and V is the volume of the test solution (l).

3. Results and Discussion

3.1. Factors affecting the adsorption rate

3.1.1. Effect of pH

It is known that the pH of the test solutions has a major impact on the adsorption and removal of metal ions from aqueous solutions. The availability of binding sites on the adsorbent is significantly affected by the metal chemistry in relation to pH in the solution [7]. Equilibrium experiments were carried out at pH ranging from 2.0 to 8.0 in order to determine the impact of this parameter on the adsorption of the copper and lead ions by flyash. Aliquots of dilute NaOH and/or HCl solution were added to the test solution, to adjust the pH of the metal ions (100 mg/I) and the solutions were treated with 1.0 g fly ash and kept in contact for 30 min at a temperature of 303 ^{o}K. The initial copper and lead ions concentrations (100 mg/l) and adsorption time were retained [8]. Figure 1 shows the effect of the initial pH on the adsorption of copper and lead metal ions on fly ash. The % removal of copper and lead ions increased by increasing the pH of the test solution from pH 2.0 to 8.0, reaching a maximum adsorption capacity at pH 6.0. In acidic medium, however, a weak adsorption occurs due to the competition between the protons on fly ash silica (≡Si-OH) and the metal cations. However, The high adsorption at high pH values may be attributed to the presence of free lone pair of electrons (≡Si-O¨), suitable for coordination with the metal ions. The metal ions can generally be solved and hydrolyzed in an aqueous solution [9,10]. The optimal pH values for maximum adsorption copper and lead ions by fly ash was found to be 6.0 and 7.0, respectively

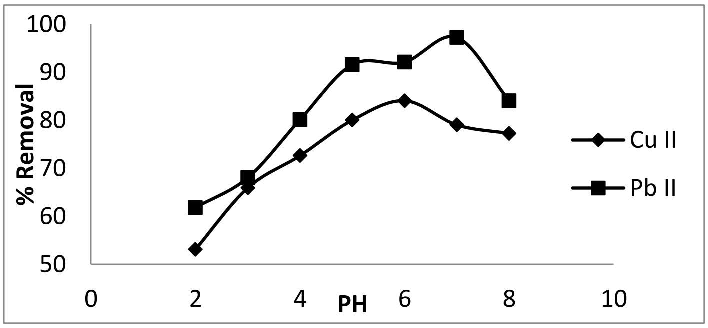

Figure1. Effect of pH on the adsorption of copper and lead ions onto fly ash (the initial metal concentration =100 mg/l, fly ash dose =1.0 g, stirring speed = 600 rpm, T=303 ^{o}K and contact time = 30 min).

3.1.2. Effect of contact time

The adsorption of copper and lead ions was plotted over different time intervals and shown in Figures 3 – 6). The adsorption effectiveness was calculated on the basis of the change in metal concentration in the aqueous solution before and after adsorption equilibrium using five different initial concentrations of flying ash (50, 100, 150, 200,300 mg/l) and 1.0 g/l metal ion solution. For all concentrations of metal and fly ash studied, adsorption capacity was almost constant, and was therefore considered as the equilibrium state. The initial speed may be due to surface adsorption, where the adsorbent surface is free during initial stages [11]. Then the reactions continue at a faster rate, after which, adsorbed metal ions penetrate through the adsorbent pores, which is called intra-particle diffusion, and adsorbed into the pore. [12]. Many sites were gradually available for both the sorption process and the adsorption equilibrium. From these plots, it is clear that the amount of metal adsorption increases with increasing the contact time at all initial metal concentrations reaching an equilibrium within 30 minutes [13].

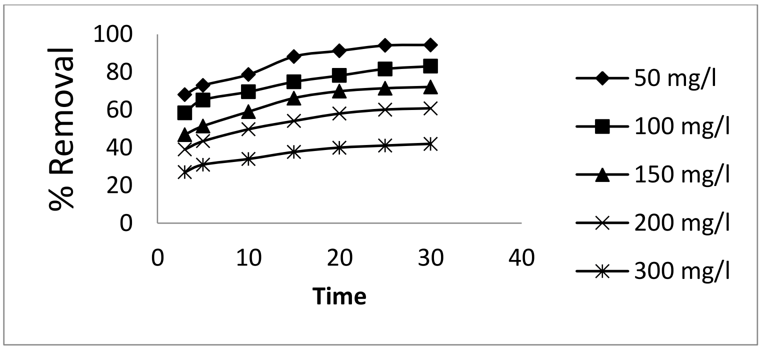

Figure 2. Effect of contact time for adsorption of copper onto fly ash (initial copper ion concentration = 50 to 300 mg/l, fly ash dose =1.0 g/l, pH = 6, stirring speed =600 rpm, contact time = 30 min and T= 303 ^{o}K).

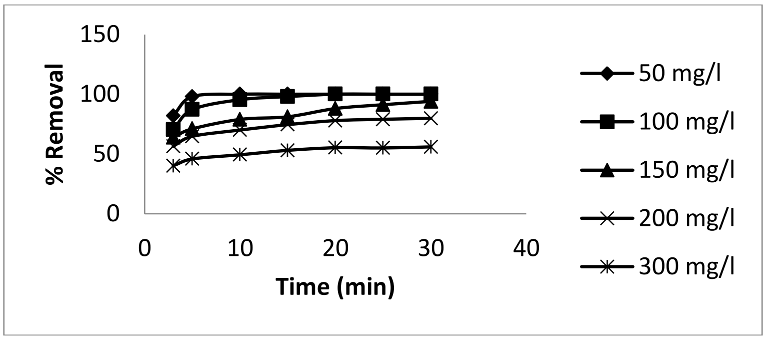

Figure 3. Effect of contact time on the adsorption of lead ions onto fly ash (initial lead ion concentration = 50 to 300 mg/l, fly ash carbon dose =1.0 g/l, pH = 7, stirring speed =200 rpm, contact time = 30 min and T= 303 ^{o}K).

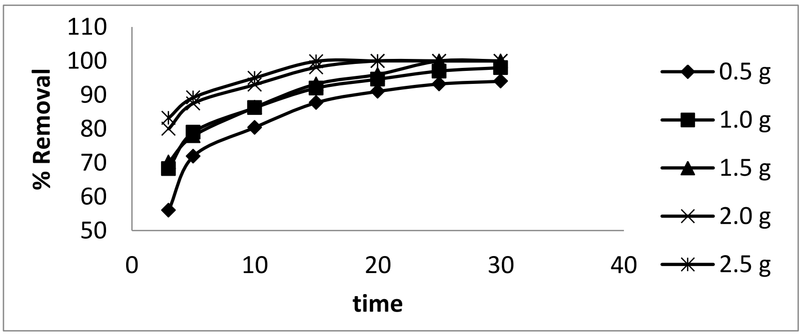

Figure 4. Relation between % metal ions removal and contact time with different doses of fly ash at 200 rpm, 303 ^{o}K and initial concentration of 100 ppm copper ions.

In addition, it is observed that the amount of metal ion uptake, q_t (mg/g) increases with the increase of the initial concentration of metal ions. This kinetic experiment clearly indicates that the adsorption of copper and lead metal ion by the fly ash carbon is a more or less two-step process; a very rapid adsorption of the metal ions on the outer surface of the adsorbent followed by possible slow intra-particle diffusion in the inner part of the adsorbent. This two-stage metal ion uptake has been suggested for other adsorption process [14].

3.1.3. Effect of adsorbent dose

The dependence of copper and lead ions adsorption on the different dose of fly ash carbon (0.5 to 2.5 g/l), while keeping other parameters (pH, agitation speed, temperature, initial copper and lead ions concentration and contact time) constant were investigated. Figures 4 and 5 show that when the adsorption dose of fly ash was increased from 0.5 to 2.5 g/l, the percent metal removal increased from 49% to 96% for copper ions and from 56% to 100% for lead ions. The optimal adsorbent dosage for copper and lead ions removal using fly ash carbon is 1.0 g/l. In agreement with other work [15,16], the constant initial concentration, the sum of adsorbed metal ions decreases as the dose of the adsorbate increases.

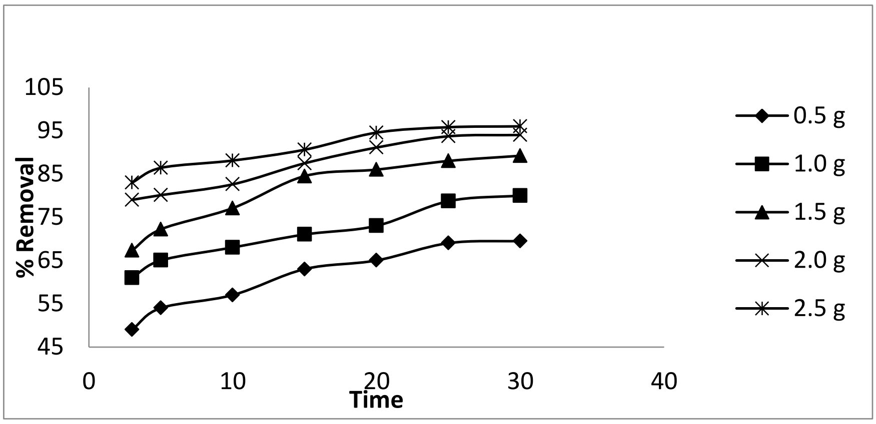

Figure 5. Relation between % metal ions removal and time with different doses of fly ash at 600 rpm, 303 ^{o}K and initial concentration 100 ppm of lead ions.

3.1.4. Effect of initial copper and lead ions concentration

The removal of copper and lead ions from aqueous solutions was significantly influenced by the initial concentration of the metal ions [17,18]. The removal percent of both ions decreases from 100 to 42 % with the increase of the initial metal ions concentrations from 50 ppm to 300 ppm. At lower metal ions concentrations, the ratio of the available adsorption sites to the initial concentration of copper and lead ions are high causing complete adsorption. However, at higher metal ions concentrations, the available adsorption sites decreased compared to the concentration of the metal ions present in the solution due to lack of sufficient active sites on fly ash, and thus, the percentage sorption of metals decreased. The amount of metal ions, q_e (mg/g), increased with increasing their initial concentration as shown in Figure 6.

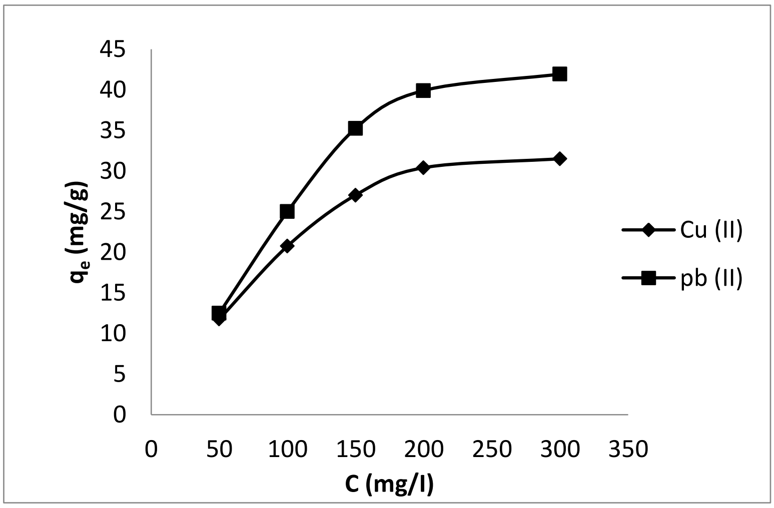

Figure.6. Relation between q_e and initial concentration for copper and lead ions.

3.1.5. Effect of temperature

It has been reported that increasing the temperature reduces the viscosity of the solution, which increases the rate of diffusion of the adsorbate ions through the external boundary layer of the adsorbent, resulting in an increase in the adsorption process [19]. Batch adsorption experiments of copper and lead ions on fly ash were carried out at temperatures of 303, 313, 323 and 333 ^{o}K and the results are shown in Figures (8, 9). The increase in temperature leads to an increase of the mobility of the metal ions and decreasing in the retarding forces acting on the ion diffusion. Furthermore, the adsorption capacity of the adsorbent increases due to fast chemical interaction between adsorbate and adsorbent and development of active surface centers. An enhanced rate of intra-particle diffusion of copper and lead ions into the pores of the adsorbent at higher temperature may be also considered [20]. This suggests that the adsorption process proceeds through an endothermic mechanism [21,22]. Changes in many thermodynamic parameters are linked to the temperature dependence of the adsorption method. The important thermodynamic properties such as standard Gibbs free energy (ΔG^o), standard enthalpy change (ΔH^o), and standard entropy change (ΔS^o) were calculated using the adsorption equilibrium data obtained at various temperatures. The following equations were used to estimate these parameters:

$$4.\ K_e = \frac{q_e}{C_e} \qquad (4)$$

$$\Delta G^o = -RT \ln K_e \qquad (5)$$

$$\Delta G^o = \Delta H^o - T\Delta S^o \qquad (6)$$

$$\ln K_e = \frac{\Delta S^o}{R} - \frac{\Delta H^o}{RT} \qquad (7)$$

Where q_e (mg/g) is the quantity of copper and lead ions adsorbed onto the fly ash from the test solution at equilibrium, C_e (mg/l) the equilibrium concentration of copper and lead ions in the solution, R (J/mol.K) the gas constant 8.314, T (^{o}K) the absolute temperature, and K_e (l/g) the adsorption equilibrium constant. ΔH^o and ΔS^o were obtained from the slope and intercept of the van’t Hoff’s plot of ln (K_e) *versus 1/T* as shown in Figure10. The values of ΔG^o, ΔH^o, and ΔS^o are collected in Table (1).

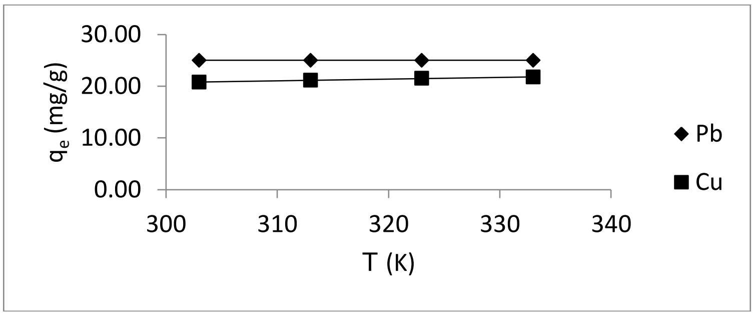

Figure 7. Relation between q_e and temperature at constant initial metal ions concentration (100 mg/l, 1.0 g/l dose of fly ash and 600 rpm.

From the data obtained, it can be observed that the Gibbs free energy of copper and lead ions adsorption onto fly ash carbon decreased with increasing temperatures, its value was negative at all tested temperatures. This means that temperature is needed for the adsorption process. The positive value of ΔH^o indicates that the adsorption mechanism is endothermic, and the negative Gibbs' free energy (ΔG^o) values confirm that the adsorption of copper and lead ions is temperature dependent. At high temperature, the metal ions are readily adsorbed due to the high adsorption rate and capacity in the equilibrium time [84]. The positive ΔS^o suggests an increase in randomness at solid / liquid interface during the adsorption of copper and lead, thus allowing the prevalence of randomness in the system [20-24]. Figure 9 shows that the increase in temperature is associated with an increases in the adsorbed copper and lead ions This also indicates that the adsorption mechanism is endothermic and may be attributed to the increase of ions mobility, which increases the amount of ions that interact with active sites at the adsorbent surfaces. Other researchers have found similar patterns in aqueous phase adsorption. The entropic term ΔS^o is the dominant factor in determining the sign of ΔG^o, as shown in equation (6). Furthermore, the negative values of $\Delta G°$ demonstrate the spontaneous behavior of the sorption processes [25]. The decrease in the value of $\Delta G°$ with the increase of temperature shows that the reaction is more spontaneous at higher temperature. Consequently the overall adsorption process of copper and lead ions on fly ash proceeds through an intra-particle diffusion [26].

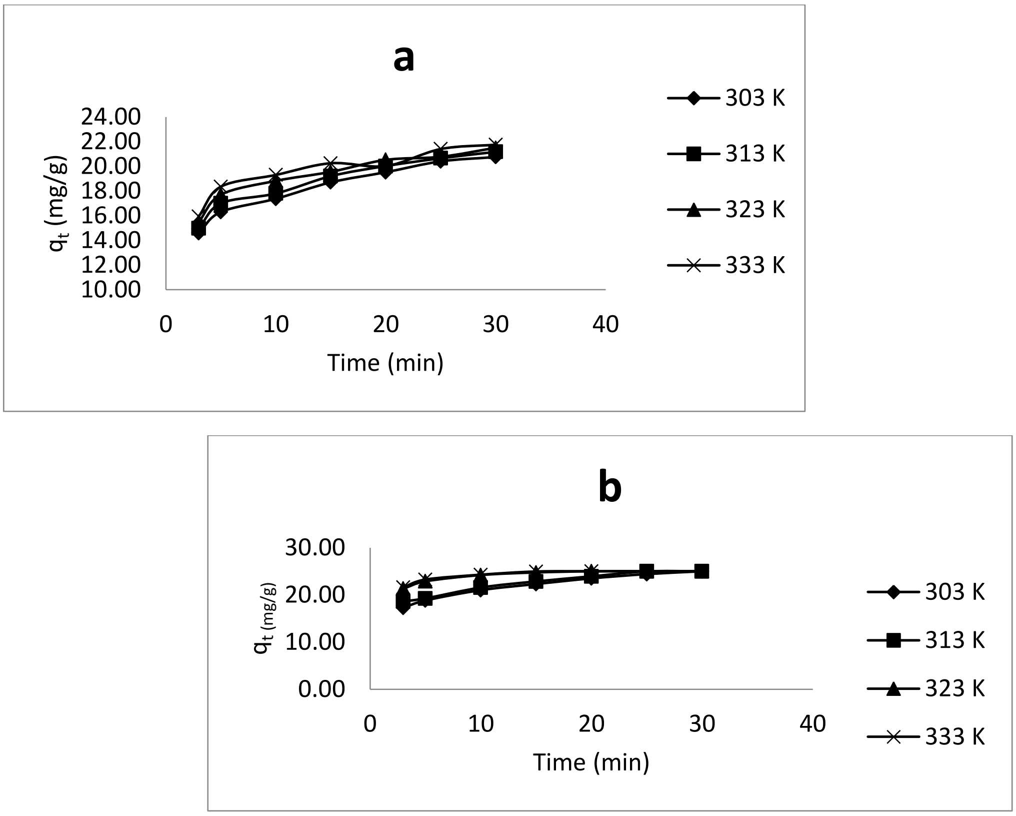

Figure 8. Relationship between q_t and contact time at different temperatures, constant initial metal ions concentration of 100 mg/l, 1.0 g/l dose of fly ash and 200 rpm. a) copper b) lead ions.

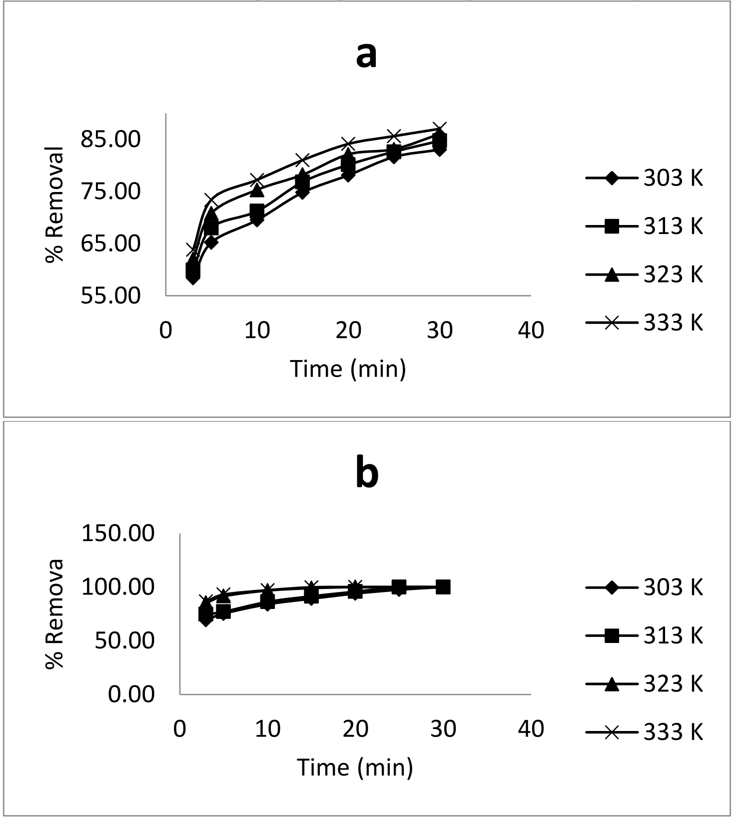

Figure 9. Relationship between % of metal removal and contact time at different temperatures, constant initial metal ions concentration of 100 mg/l, 1.0 g/l dose of fly ash and 600 rpm a) copper b) lead ions.

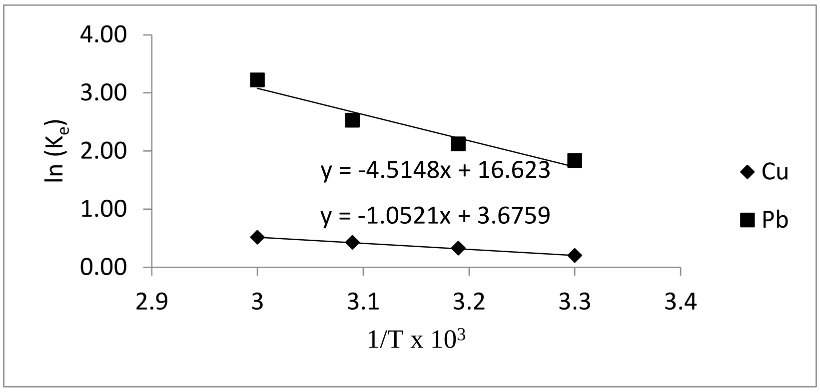

Figure 10. Relationship between ln (K_e) and reciprocal of temperature, at constant initial metal ions concentration of 100 mg/l, 1.0 g/l dose of fly ash and 600 rpm for copper and lead ions

Table (1): Thermodynamic parameters of copper and lead ions onto fly ash at constant initial metal ions concentration (100 mg/l).

Heavy metal	**T**	**Thermodynamic parameters**		
	(°K)	**ΔG^o (kJ/mol)**	**ΔH^o (kJ/mol)**	**ΔS^o (J/mol.K)**
Copper ions				
	303	-502.06		
	313	-844.96	-1.052	3.675
	323	-1152.04		
	333	-1424.86		
Lead ions				
	303	-1525.90		
	313	-1955.72	-4.51	16.62
	323	-2488.12		
	333	-3236.53		

3.2. Adsorption kinetics

Kinetic models are commonly used to understand and explain the nature of the adsorption processes and to evaluate the efficiency of adsorbents of copper and lead ions on fly ash. Thus, Lagergren pseudo-first-order [27], and pseudo-second-order [28, 29] were tested. Correlation coefficients were used to express the consistency between the obtained experimental results and model-predicted values (R^2, values close or equal to 1, the relatively higher value is the more applicable model). Figures 2 and 3 show good removal of copper and lead ions by adsorption as a function of contact time for various initial metal concentrations (50, 100, 150, 200, and 300 mg/l) during the first 30 minutes of contact with fly ash showed good adsorptive results. With contact time above 30 minutes, there was no increase in adsorption. These findings show that the actual adsorption of metal ion and binding to the adsorbent are extremely fast. Two kinetic models, including pseudo-first and pseudo-second orders, are used to examine the experimental data and to investigate the mechanism of adsorption. The possible rate-controlling measures, which involve mass transport and chemical reaction processes are also examined. The adsorption mechanism of copper and lead ions in the solid phase is explained by a good correlation of the kinetic data (Table 2). The R^2 values are compared to determine the validity of each of the examined model. As a result, the adsorption of copper and lead ions perfectly matches the pseudo-second order model, as shown in Table 2. The measured equilibrium adsorption potential is similar to the experimental results with high correlation coefficients ($R^2 > 0.998$).

3.2.1. The pseudo first-order kinetic model

The Lgergren pseudo-first-order model [27] is the earliest known equation which describes the adsorption rate as a function of the adsorption capacity.

$$\ln(q_e - q_t) = \ln(q_e) - k_1 t \qquad (8)$$

Where q_e (mg/g) and q_t (mg/g) are the amounts adsorbed per unit mass at equilibrium at any time, t (min) is time, and k_1 is the pseudo first order adsorption rate coefficient. The slope and intercept of the linear plot of ln (q_e-q_t) *vs. t* yield the values of k_1 and q_e, shown in Figures (11, 12) and Table (2). The value of q_e must be known in order to match the experimental data to equation (8). A comparison of experimentally determined q_e values with those obtained from plots of ln (q_e-q_t) *vs t* [27, 28] is the real test of equation (8) validity. The correlation coefficients of pseudo first-order kinetic model are low and the difference of equilibrium adsorption capacity (q_e) between the experimental and the calculated data was observed, indicating a poor pseudo first-order fit to the experimental data.

3.2.2. The pseudo second-order kinetic model

The present kinetic data, are based on the assumption that the adsorption process follows pseudo second-order.

$$t/q\_t = 1/(k\_2\, q\_e \hat{}\, 2) + 1/q\_e\ t \qquad (9)$$

Where k^2 is the adsorption pseudo-second order rate constant (mg g^{-1} min^{-1}). The plot of *t/qt versus t* is linear (Figures 18, 19) with slopes and intercepts usable for determining q_e and k_2 (q_e=1/slope and k_2 = (slope)^2/intercept, respectively. Each linear plot was used to examine the applicability of the above two models shown in Figures (13, 14). The correlation coefficient, R^2, is calculated from these plots to quantify the applicability of each model. Table 1 shows the kinetic rate constants obtained from the first and second-order pseudo kinetic models (2). The pseudo-second order adsorption model's correlation coefficient, R^2, is relatively high (> 0.9979), and the adsorption capacities calculated by the model are also close to those experimently obtained. The R^2 values for the pseudo-first order, on the other hand, are not satisfactory. As a result, the pseudo-second order adsorption model is more suitable for describing copper and lead ions adsorption kinetics on fly ash In general, the adsorption reaction is known to proceed through the following three steps: (i) transfer (diffusion) of adsorbate from the bulk solution to adsorbent surface, (ii) migration of adsorbate into the pores of adsorbate and (iii) interaction of adsorbate with the available sites on the interior surface of pores [30].

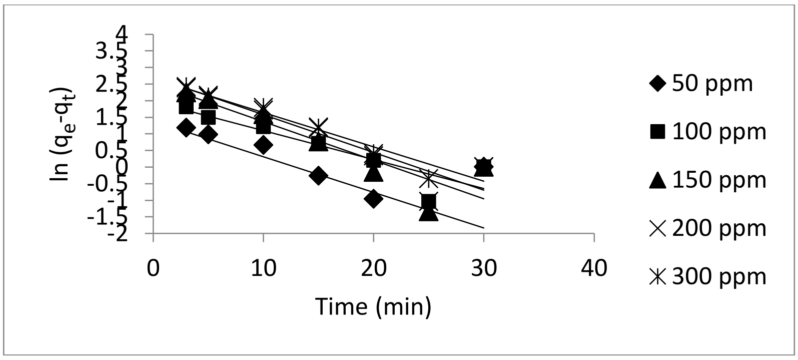

Figure 11. Pseudo-first order kinetic fit for the adsorption of copper ions onto fly ash at different initial concentrations, 1.0 g fly ash dose, 600 rpm and 303 °K.

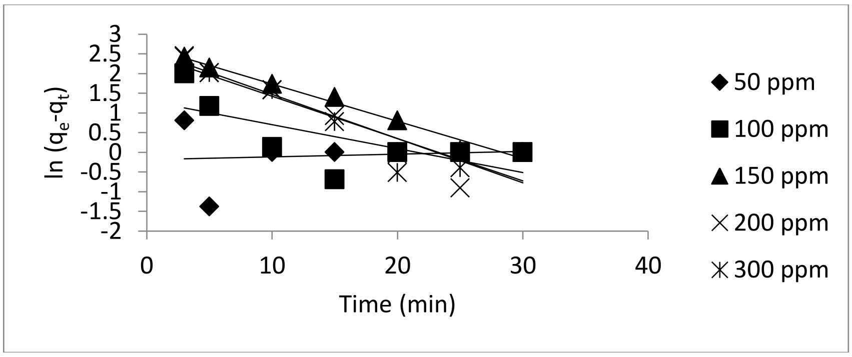

Figure 12. Pseudo-first order kinetic fit for the adsorption of lead metal ion onto fly ash at different initial concentration, 1.0 g fly ash dose, 200 rpm and 303 ^{0}K.

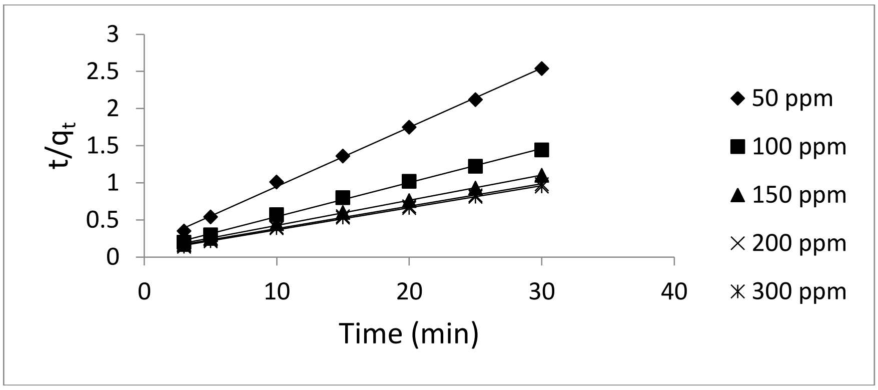

Figure 13. Pseudo-second order kinetic fit for the adsorption of copper ions onto fly ash at different initial concentrations, 1.0 g fly ash dose, 200 rpm and 303 ^{o}K.

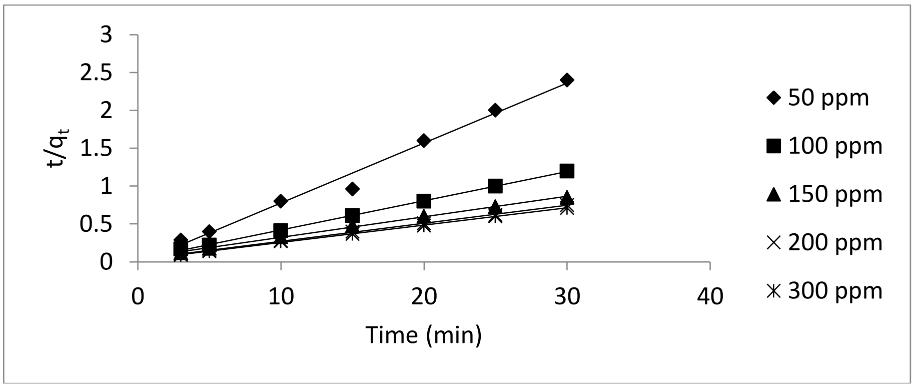

Figure 14. Pseudo-second order kinetic fit for the adsorption of lead metal ion onto fly ash at different initial concentration, 1.0 g fly ash dose, 600 rpm and 303 ^{o}K.

Table (2): Kinetic models and other parameter for adsorption of a) copper b) lead ions onto fly ash at different initial concentrations of metal ions, 1.0 g dose, 600 rpm, 303 ^{o}k.

(a)

Kinetic models	parameters	Concentration of copper ion solution, (mg/l)				
		50	100	150	200	300
	q_e(Exp) (mg/g)	11.78	20.75	27.03	30.40	31.50
Pseudo-first order equation	q_e (calc.)(mg/g)	1.3816	1.9731	2.5237	2.7199	2.8712
	k_1(min^{-1})	-0.1072	-0.0873	-0.1159	-0.1139	-0.1033
	R^2	0.9417	0.9027	0.9731	0.8777	0.9051
Pseudo-second order equation	q_e (calc.) (mg/g)	12.54	21.83	29.41	33.11	33.67
	k_2(g/mg.min)	0.0420	0.0241	0.0136	0.0114	0.0127
	$k_2q_e^2$(mg/g.min)					
	$k_2q_e^2$					
	$t_{0.5}$					
	R^2	0.9984	0.9977	0.9986	0.9989	0.9976

(b)

Kinetic models	Parameters	Concentration of lead ions solution. (mg/l)				
		50	100	150	200	300
Pseudo-first order equation	q_e(Exp) (mg/g)	12.5	25.0	35.2	39.9	41.92
	q_e (calc.)(mg/g)	0.1894	1.3087	2.6802	2.5941	2.4962
	k_1(min^{-1})	0.0078	-0.0607	-0.0945	-0.1124	-0.1073
	R^2	0.012	0.4649	0.978	0.8578	0.8326
Pseudo-second order equation	q_e (calc.) (mg/g)	12.62	25.90	36.90	42.01	43.85
	k_2(g/mg.min)	0.4417	0.0424	0.0142	0.0164	0.0183
	$k_2q_e^2$(mg/g.min)					
	$k_2q_e^2$					
	$t_{0.5}$					
	R^2	0.9861	0.9993	0.9978	0.9992	0.9992

3.3. Equilibrium adsorption study

The design and optimization of adsorption processes require the development of an appropriate isotherm model. Langmuir, Freundlich, Redlich–Peterson, Dubinin–Radushkevich, Sips, and Temkin are some of the isotherm models that have been developed for determining the equilibrium adsorption of different components from solutions[38]. Because the Langmuir, Freundlich, and Dubinin–Radushkevich equations are the most commonly used to investigate the adsorption isotherm, the experimental results of this study were applied with these two models. Equilibrium adsorption isotherms are useful for determining the adsorption capacity of copper and lead ions as well as diagnosing the nature of adsorption on fly ash [39].

3.3.1. Langmuir model

Adsorption of a solute from a liquid solution as monolayer adsorption on a surface with a finite number of identical sites is commonly expressed by the theoretical Langmuir sorption isotherm [38] The Langmuir isotherm model assumes uniform adsorption energies on the surface with no adsorbate transmigration in the plane of the surface. For estimating the maximum adsorption capacity corresponding to complete mono-layer coverage on the sorbent surface, the Langmuir isotherm model was chosen. The linear representation of the

Langmuir isotherm model is expressed as follows [38].

$$\frac{C_e}{q_e} = \frac{1}{q_{max} \cdot b} + \frac{C_e}{q_{max}} \qquad (10)$$

Where q_e is the adsorbent's equilibrium, metal ion concentration (mg/g), C_e is the solution's equilibrium metal ion concentration, q_{max} is the adsorbent's monolayer adsorption saturation capacity, and b is the Langmuir constant. Figure 15 depicts linear plots of C_e/q_e *vs* C_e and is used to calculate the Langmuir isotherm parameters with a linear regression equation and the results are tabulated in Table (3). The slope and intercept of the plots are used to calculate b and q_{max}, respectively. High R^2 values for copper and lead metal ions reveal extremely good application of Langmuir model to these adsorptions.

The Langmuir isotherm's can be expressed in terms of a dimensionless constant separation factor (R_L), which is defined as:

$$\boldsymbol{R_L = \frac{1}{1+bC_o}} \qquad (11)$$

Where C_o is the initial concentration of the metal ion. The values of R_L indicate the type of isotherm to be either unfavorable ($R_L > 1$), linear ($R_L = 1$), favorable ($0 < R_L < 1$) or irreversible ($R_L = 0$). From this study R_L, values for Cu ions adsorption ranged from 2.5 to 10.1 and for Pb ions adsorption ranged from 0.23 to 1.06. Therefore, the adsorption process is favorable and fit with this model [39,40].

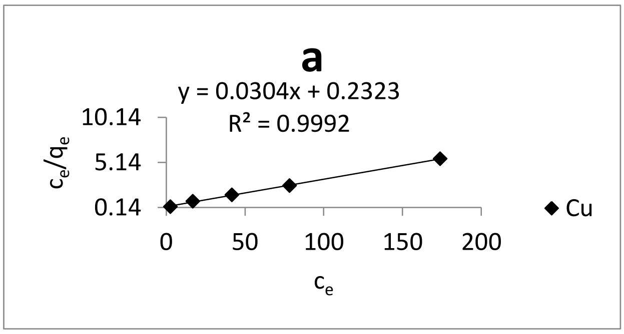

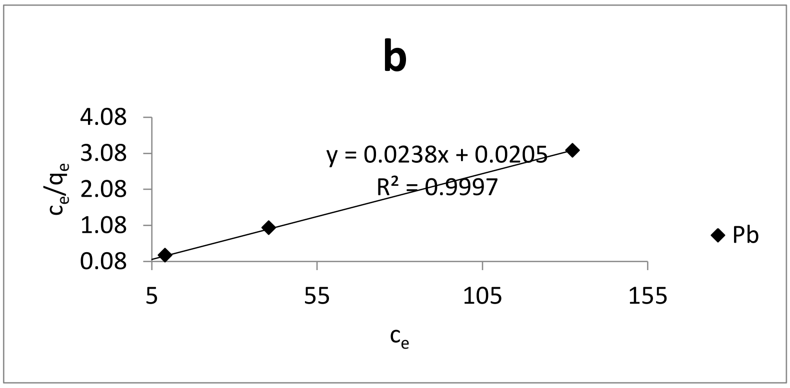

Figure.15. Linear Langmuir adsorption isotherm for a) copper, b) lead (II) ions with fly ash at 303 ^{o}K.

3.3.2. Freundlich model

The Freundlich isotherm model [42] is applicable to adsorption on heterogeneous surfaces with interactions between adsorbed molecules. The Freundlich equation suggests that sorption energy decreases exponentially as an adsorbent's sorption centers are completed. This isotherm is an empirical equation that can be used to describe heterogeneous systems and is written in linear form as follow

$$\log q_e = \log K_f + \frac{1}{n} \log C_e \qquad (12)$$

The Freundlich constants K_F and $1/n$ denote the adsorption capacity and intensity, respectively. The constants $1/n$ and K_F are calculated from the slope and intercept, respectively, and collected in Table 21. The results show the linear plot of log q_e versus log C_e (3). Since the obtained value of $1/n$ is less than 1, this indicates favorable adsorption and confirms the adsorbent's heterogeneity (Figure 16). Moreover, this suggests formation of strong bonds between copper and lead ions and fly ash [43].

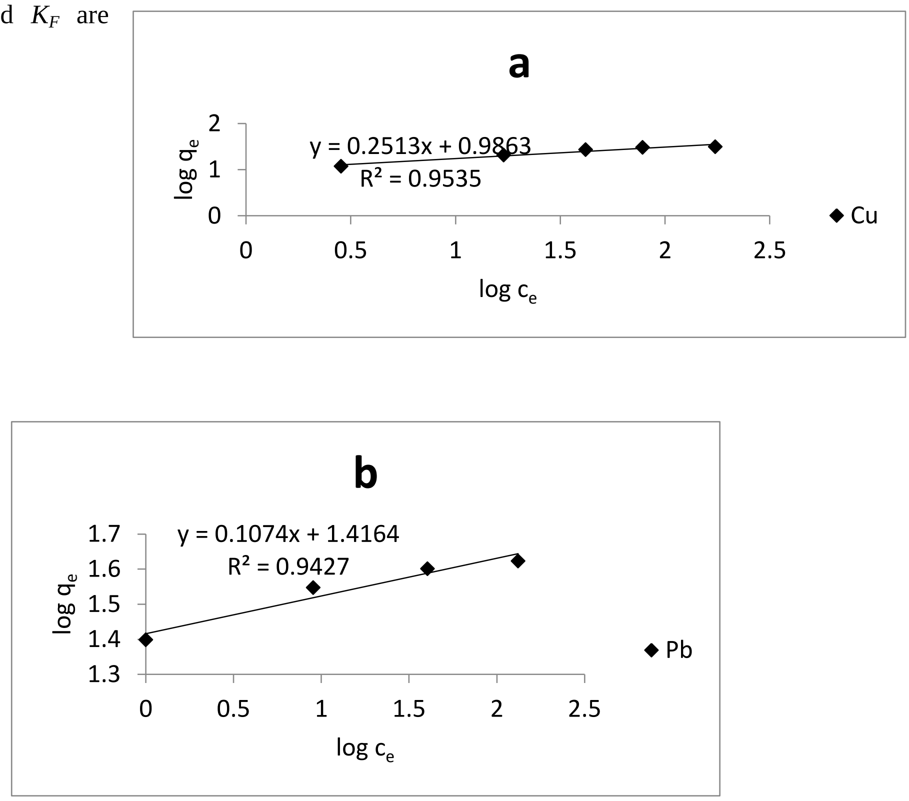

Figure 16.Linear Freundlich adsorption isotherm for a) copper, b) lead ions with fly ash at 303 ^{o}K.

3.3.3. Dubinin–Radushkevich (D-R) isotherm model

The D–R isotherm model is a semi-empirical equation in which a pore filling mechanism governs adsorption. It assumes that the adsorption proceeds in multilayered, that van der Waals forces are involved, and that it can be applied to physical adsorption processes [44]. The D–R isotherm model is written in a linear form as:

$$\ln q_e = \ln q_s - K_{ad}\varepsilon^2 \quad (13)$$

Where, q_s is the theoretical isotherm saturation capacity (mg/g), K_{ad} is the D-R isotherm constant (mol^2/J^2) and ε is the Polanyi potential which is equal to $RT \ln\left(1 + \frac{1}{C_e}\right)$, where R (J/mol.K) is the gas constant and T (K) is the absolute temperature. Figure 17, shows a linear relation between ln q_e versus ε^2. The slope of the plot gives K_{ad} (mol^2/J^2) and the intercept yields the sorption capacity q_s (mg/g) [Table (4)]. The constant K_{ad} gives an idea about the mean free energy E (kJ/mol) for adsorption per molecule of adsorbate when it is transferred to the surface of the solid from infinity in the solution and can be calculated using the relationship:

$$E = 1 / (2\, k_{ad})^{1/2} \quad (14)$$

This parameter indicates whether the adsorption mechanism is chemical ion-exchange or physical interaction. When E value lies between 8 and 16 kJ/mol, the adsorption process is considered as chemical ion-exchange, whereas when E value is less than 8 kJ/mol, the adsorption process is physical interaction. In the case of copper, the adsorption of the mean free energy is 100 kJ/mol, while in the case of lead, it is 235 kJ/mol, which corresponds to a physical adsorption mechanism [25, 32-33]. All of the isotherm models fit very well with adsorption process and R^2 values are compared in Table (3).

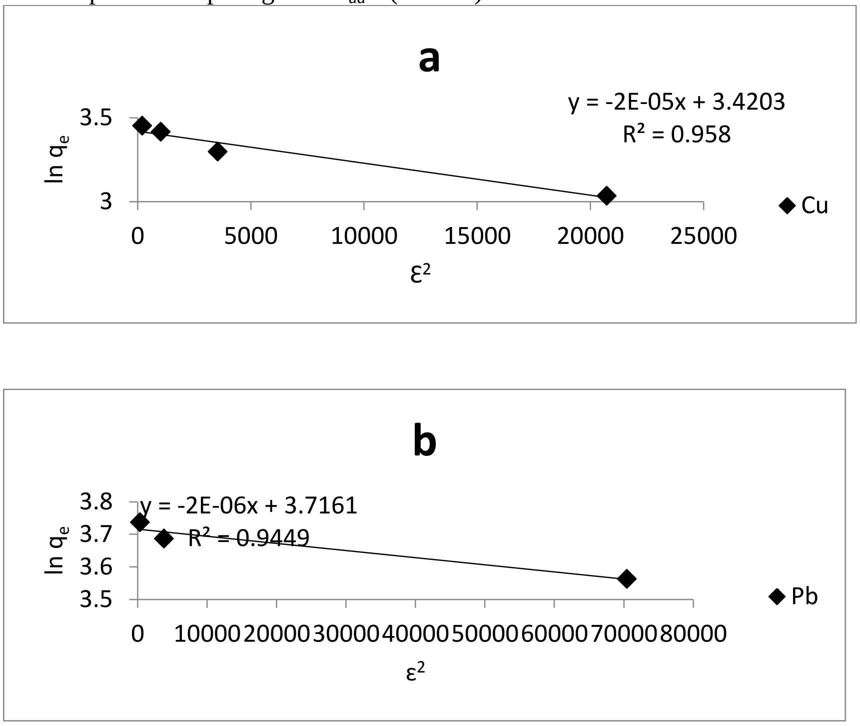

Figure17. The Dubinin–Radushkevich (D-R) adsorption isotherm for a) copper, b) lead ions with fly ash at 303 °K.

Table (3). Adsorption isotherm constants for the adsorption of copper and lead ions onto fly ash at 303 °K.

(a)

C_o (mg/l)	Copper ions										
	Langmuir				Freundlish			Dubinin-Radushkevich			
	q_{max} (mg/g)	b (dm^3/mg)	R^2	R_L	$1/n$	K_f	R^2	ε	K_{ad}	E (kJ/mol)	R^2

50	0.2323	0.0304	0.9992	2.50	0.2513	0.986	0.9535	757.642	$-2x10^{-5}$	100	0.958
100				4.04				143.99			
150				5.56				59.486			
200				7.08				31.928			
300				10.1				14.436			

(b)

C_o (mg/l)	Lead ions										
	Langmuir				Freundlish			Dubinin-Radushkevich			
	q_{max} (mg/g)	b (dm^3/mg)	R^2	R_L	$1/n$	K_f	R^2	ε	K_{ad}	E (kJ/mol)	R^2
50	0.0205	0.0238	0.9997	0.5494	0.1074	1.4127	0.9427	0.0	$-2x10^{-6}$	100	0.9449
100				0.3787				0.0			
150				0.2890				265.4			
200				0.2336				61.50			
300				1.0689				18.96			

3.4 Scanning electron microscopy (SEM)

SEM examination is widely used to investigate the morphological characteristics and surface properties of adsorbent materials [41,42]. SEM is used in this study to assess the morphological changes in fly ash surfaces as a result of copper (II) and lead (II) ion adsorption. Scanning electron microscopy was used to examine the morphology of three different types of fly ash particles, and the results are shown in Figure 18. The surface of these samples (Figure 23 A) shows a distinct roughness with more curved planes, porous and holes structure. The SEM micrographs displays macro pores in the fly ash (Figure 18 A) with large surface area which enable metal adsorption with high efficiency. Figures (18 B, C) show that the surface morphology of fly ash has undertaken significant changes after adsorption of copper and lead ions. The SEM image of 1.0 g fly ash and 250 mg/l solution at 303 ^{o}K and 600 rpm for 30 min (23 B) shows that interlayer spaces have collapsed, resulting in tightly packed flakes and a more tightly bound structure. With another dose of fly ash (1.0 g); the external surface of the fly ash is fully saturated with rough cavities. This phenomenon revealed that the adsorption process involved a multi- layer of coverage on the fly ash surface [42].

Figure18. SEM micrographs of the fly ash A) before adsorption of copper and lead ions B) after

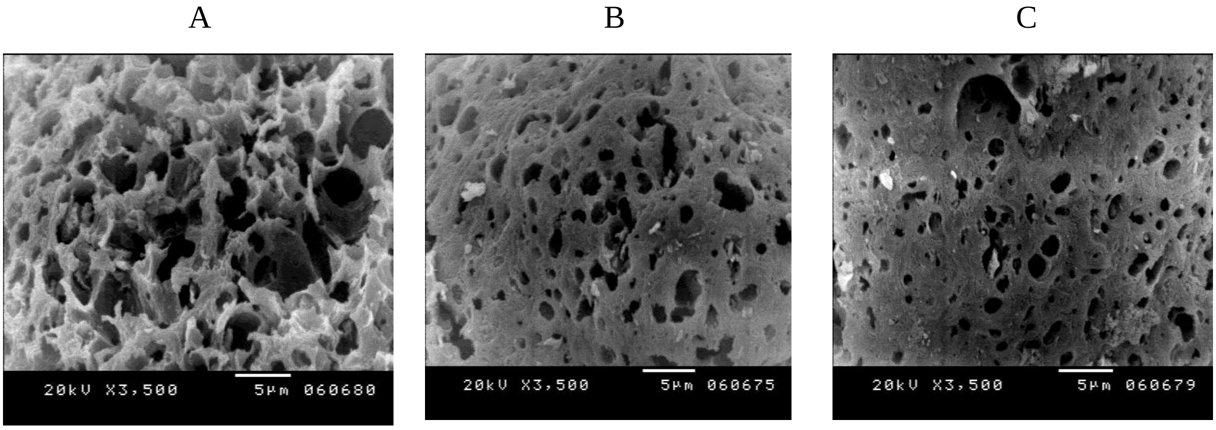

---

adsorption of copper ions C) after adsorption of lead ions.

3.5 X-Ray diffraction

The diffractogram of fly ash samples before and after copper and lead ions adsorption are shown in Figure 19. These graphs show the relation between diffracted intensity and diffraction angle and confirm the crystallinity pattern. The results show that adsorption of copper and lead ions on fly ash has no significant effect on the crystalline structure of fly ash. The main difference in the XRD patterns of fly ash is the intensity of the first order diffraction peak. This difference is probably due to the different adsorption coefficients of the elements present on fly ash or due to the transformation of amorphous fly ash carbon leading to an increase of the graphitization degree after adsorption of the copper and lead ions on fly ash [42].

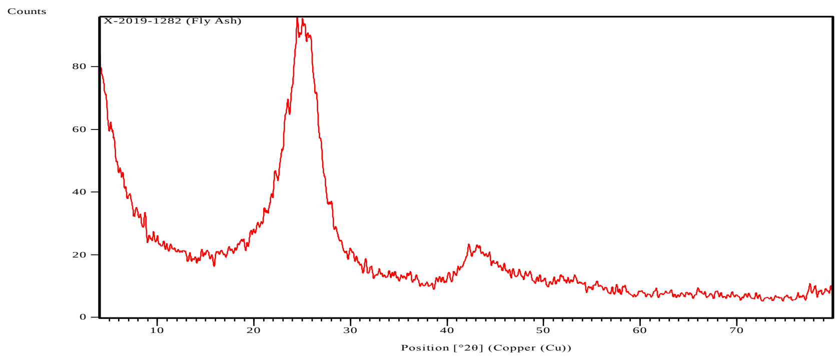

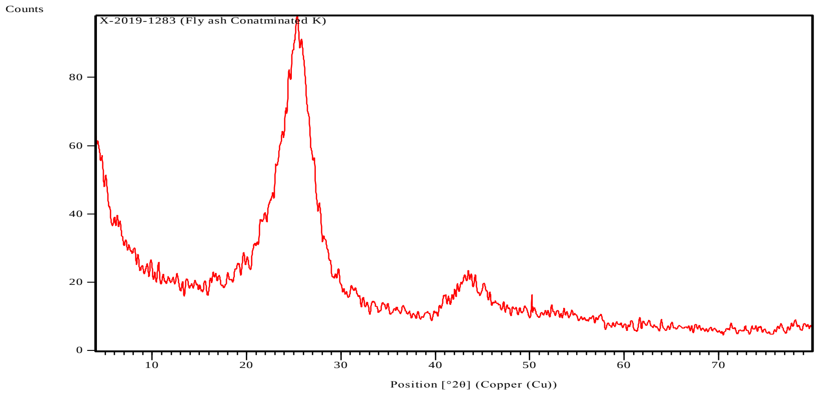

Figure 19. XRD fly ash before and after removal of copper and lead ions.

3.6. Adsorbate recycling/ reusability and metal ions recovery

A preliminary study reveals possible metal ion recovery by leaching for at least one hour with 5 M hydrochloric acid solution. However, the adsorption capacity of fly ash deteriorate. A more simple approach is to incinerate the metal loaded adsorbate above 600^{o}C to convert the adsorbate into carbon dioxide and water and the metal ions into metal oxides, followed by dissolving the metal oxides residue in 5% hydrochloric acid to obtain metal chlorides solution. Other leaching agents are under investigation.

3.7. Conclusions

Fly ash is an environmental hazard worldwide, and it poses a threat to ecosystems, including people, animals and plants. The present study presents a suitable and convenient low cost application of the use of fly ash for industrial water treatment and for the removal of copper and lead ions from aqueous waste water. Detailed physicochemical study and mechanism of the removal of 95 – 100 % of the initial copper and lead ions from aqueous solutions by adsorption on fly ash are described. Adsorption factors affecting the removal process including the effect of metal ions concentrations, contact time, temperature, fly ash dose and pH are examined.

References

1- Mishra, S., Bharagava, R.N., More, N., Yadav, A., Zainith, S., Mani, S. and Chowdhary, P., Heavy metal contamination: an alarming threat to environment and human health. In *Environmental biotechnology: For sustainable future* . Springer, Singapore. (pp. 103-125) (2019).

2- Meena, A.K., Mishra, G.K., Rai, P.K., Rajagopal, C. and Nagar, P.N., Removal of heavy metal ions from aqueous solutions using carbon aerogel as an adsorbent. *Journal of hazardous materials*, *122*(1-2), pp.161-170(2005).

3- Rios, Carlos A., Craig D. Williams, and Clive L. Roberts. "Removal of heavy metals from acid mine drainage (AMD) using coal fly ash, natural clinker and synthetic zeolites." Journal of Hazardous Materials 156.1-3: 23-35 (2008)

4- Xhixha, G., Bezzon, G.P., Broggini, C., Buso, G.P., Caciolli, A., Callegari, I., De Bianchi, S., Fiorentini, G., Guastaldi, E., Xhixha, M.K. and Mantovani, F., The worldwide NORM production and a fully automated gamma-ray spectrometer for their characterization. *Journal of Radioanalytical and Nuclear Chemistry*, *295*(1), pp.445-457 (2013)

5- Villaescusa, I., Fiol, N., Martínez, M., Miralles, N., Poch, J. and Serarols, J.,. Removal of copper and nickel ions from aqueous solutions by grape stalks wastes. *Water research*, *38*(4), pp.992-1002 (2004)

6- Rohlich, Gerard A. "Drinking Water and Health." Safe Drinking Water: Current and Future Problems : 47-75 (2016)

7- Owa, F. D. "Water pollution: Sources, effects, control and management." Mediterranean Journal of Social Sciences 4.8: 65 (2013)

8- J. K. Edzwald, Water Quality and Treatment: A Handbook on Drinking Water, 6th ed, McGraw-Hill, (2011)

9- Abdel Rahman EM, Hassan SS, Kamel AH, El-Subruiti GM, Diab HM. Removal of Uranium-238 Ions from Contaminated Ground Water Containing NORM by Adsorption on Fly Ash Carbon: Equilibrium, Kinetic and Thermodynamic Studies. Arab Journal of Nuclear Sciences and Applications (Online), 54(2):92-103 (2021).

10- Xin, X., Wei, Q., Yang, J., Yan, L., Feng, R., Chen, G., Du, B. and Li, H., Highly efficient removal of heavy metal ions by amine-functionalized mesoporous Fe3O4 nanoparticles. Chemical Engineering Journal, 184, pp.132-140 (2012)

11- Prasad, Murari, and Sona Saxena. "Sorption mechanism of some divalent metal ions onto low-cost mineral adsorbent." Industrial Engineering Chemistry Research 43.6 1512-1522 (2004)

12- Hubicki, Zbigniew, and Dorota Kołodyńska. "Selective removal of heavy metal ions from waters and waste waters using ion exchange methods." Ion Exchange Technologies : 193-240 (2012)

13- Dickhout, J.M., Moreno, J., Biesheuvel, P.M., Boels, L., Lammertink, R.G. and de Vos, W.M. Produced water treatment by membranes: a review from a colloidal perspective. Journal of colloid and interface science, 487, pp.523-534 (2017).

14- Chauhan, G., Jadhao, P.R., Pant, K.K. and Nigam, K.D.P., Novel technologies and conventional processes for recovery of metals from waste electrical and electronic equipment: challenges & opportunities–a review. Journal of environmental chemical engineering, 6(1), pp.1288-1304 (2018)

15- Alslaibi TM, Abustan I, Ahmad MA, Foul AA. Kinetics and equilibrium adsorption of iron (II), lead (II), and copper (II) onto activated carbon prepared from olive stone waste. Desalination and water treatment. Dec 6;52(40-42):7887-97 (2014)

16- Al-Harahsheh MS, Al Zboon K, Al-Makhadmeh L, Hararah M, Mahasneh M. Fly ash based geopolymer for heavy metal removal: A case study on copper removal. Journal of Environmental Chemical Engineering. Sep 1;3(3):1669-77 (2015)

17- J. Wang and C. Chen, "Biosorbents for heavy metals removal and their future," Biotechnol. Adv., 27, 195–226, (2009)

18- Tuna, A.Ö.A., Özdemir, E., Şimşek, E.B. and Beker, U., Removal of As (V) from aqueous solution by activated carbon-based hybrid adsorbents: Impact of experimental conditions. Chemical Engineering Journal, 223, 116-128 (2013)

19- Georgieva, V.G., Gonsalvesh, L. and Tavlieva, M.P., Thermodynamics and kinetics of the removal of nickel (II) ions from aqueous solutions by biochar adsorbent made from agro-waste walnut shells. Journal of Molecular Liquids, 312, 112788 (2020)

20- Munagapati, V.S. and Kim, D.S., Equilibrium isotherms, kinetics, and thermodynamics studies for congo red adsorption using calcium alginate beads impregnated with nano-goethite. Ecotoxicology and environmental safety, 141, 226-234 (2017)

21- Schroeder, Terrence K. "Supercritical fluid enrichment of isotopes." U.S. Patent No. 7,967,893. 28 Jun. (2011)

22- GGavrilescu, Maria, Lucian Vasile Pavel, and Igor Cretescu. "Characterization and remediation of soils contaminated with thorium and potassium40." Journal of Hazardous Materials 163.2-3: 475-510 (2009)

23- Sharifipour, F., Hojati, S., Landi, A. and Faz Cano, A., Kinetics and thermodynamics of lead adsorption from aqueous solutions onto Iranian sepiolite and zeolite. International Journal of Environmental Research, 9(3),1001-1010 (2015)

24- HardiljeetBoparai, K., Joseph, M., O'Carroll, D. M., Kinetics and thermodynamics of cadmium ion removal by adsorption onto nanozerovalent iron particles, J. Hazard. Mater., vol.186, 458 (2011)

25- Bouhamed, F., Elouear, Z. and Bouzid, J., Adsorptive removal of copper (II) from aqueous solutions on activated carbon prepared from Tunisian date stones: Equilibrium, kinetics and thermodynamics. Journal of the Taiwan Institute of Chemical Engineers, 43(5), 741-749 (2012)

26- Rudzinski, W., and Wojciech, P., "Studies of the kinetics of solute adsorption at solid/solution interfaces: on the possibility of distinguishing between the diffusional and the surface reaction kinetic models by studying the pseudo-first-order kinetics." The Journal of Physical Chemistry C 111.41: 15100-15110 (2007)

27- AAzizian, Saeid. "Kinetic models of sorption: a theoretical analysis." Journal of colloid and Interface Science 276.1: 47-52 (2004).

28- Lin, Junxiong, and Lan Wang. "Comparison between linear and non-linear forms of pseudo-first-order and pseudo-second-order adsorption kinetic models for the removal of methylene blue by activated carbon." Frontiers of Environmental Science & Engineering in China 3.3: 320-324 (2009)

29- Ho, Yuh-Shan, and Gordon McKay. "Pseudo-second order model for sorption processes." Process Biochemistry 34.5: 451-465(1999)

30- Al-Anber, M.A., Removal of high-level Fe3+ from aqueous solution using natural inorganic materials: Bentonite (NB) and quartz (NQ). Desalination, 250(3), 885-891 (2010)

31- Chowdhury, Pradip, Chaitanya Bikkina, and Sasidhar Gumma. "Gas adsorption properties of the chromium-based metal organic framework MIL-101." The Journal of Physical Chemistry C 113.16: 6616-6621(2009).

32- Foo, Keng Yuen, and Bassim H. Hameed. "Insights into the modeling of adsorption isotherm systems." Chemical Engineering Journal 156.1: 2-10 (2010)

33- Afkhami, Abbas, Mohammad Saber-Tehrani, and Hasan Bagheri. "Simultaneous removal of heavy-metal ions in wastewater samples using nano-alumina modified with 2, 4-dinitrophenylhydrazine." Journal of Hazardous Materials 181.1-3: 836-844 (2010).

34- Singh, Harpreet, and Farzam Javadpour. "Langmuir slip-Langmuir sorption permeability model of shale." Fuel 164: 28-37(2016).

35- WWong, Y. C., et al. "Equilibrium studies for acid dye adsorption onto chitosan." Langmuir 19.19: 7888-7894 (2003)

36- Ho, Yuh-Shan, Wen-Ta Chiu, and Chung-Chi Wang. "Regression analysis for the sorption isotherms of basic dyes on sugarcane dust." Bioresource technology 96.11: 1285-1291 (2005)

37- Kumar, P.S., Ramalingam, S., Kirupha, S.D., Murugesan, A., Vidhyadevi, T. and Sivanesan, S., Adsorption behavior of nickel (II) onto cashew nut shell: Equilibrium, thermodynamics, kinetics, mechanism and process design. Chemical Engineering Journal, 167(1), 122-131 (2011).

38- Nguyen, C., and D. D. Do. "The Dubinin–Radushkevich equation and the underlying microscopic adsorption description." Carbon 39.9: 1327-1336 (2001)

39- Boparai, Hardiljeet K., Meera Joseph, and Denis M. O'Carroll. "Kinetics and thermodynamics of cadmium ion removal by adsorption onto nano zerovalent iron particles." Journal of Hazardous Materials 186.1: 458-465 (2011).

40- Batra, Vidya S., Sigita Urbonaite, and Gunnar Svensson. "Characterization of unburned carbon in bagasse fly ash." Fuel 87.13-14: 2972-2976 (2008)

41- Bounakhla, Moussa, and Mounia Tahri. "X-ray fluorescence analytical techniques." National Center for Energy Sciences and Nuclear Techniques (CNESTEN), Rabat, Morocco 1: 1-73 (2014)

42- Snellings, Ruben. "X-ray powder diffraction applied to cement." A practical guide to microstructural analysis of cementitious materials. CRC Press, Boca Raton 107-176(2016).